

# Dirac semimetals in group IV transition metal ditellurides

Sotirios Fragkos<sup>1,2</sup>

E. Xenogiannopoulou<sup>1</sup>, P. Tsipas<sup>1</sup>, P. Pappas<sup>1</sup>, E. Symeonidou<sup>1</sup>, Y. Panayiotatos<sup>2</sup>, P. Le Fèvre<sup>3</sup>, A. Dimoulas<sup>1</sup>

<sup>1</sup> NCSR "Demokritos", Institute of Nanoscience and Nanotechnology, 15341 Athens, Greece

<sup>2</sup> Department of Mechanical Engineering, University of West Attica, 12241 Athens, Greece

<sup>3</sup> Synchrotron SOLEIL, L'Orme des Merisiers, 91192 Gif-sur-Yvette, France

s.fragkos@inn.demokritos.gr

Topological semimetals are hosts of interesting types of low-energy quasiparticles such as type-I and type-II Dirac and Weyl fermions. Yet a type-III [1-3] emerges as a theoretical possibility exactly at the border between type-I and II (Fig. 1a), characterized by a line-like Fermi surface and a flat energy dispersion along one direction in the Brillouin Zone. We theoretically predict that 1T-HfTe<sub>2</sub> and 1T-ZrTe<sub>2</sub> transition metal dichalcogenides are type-I and type-II Dirac semimetals (Fig. 1b,c), respectively. By alloying the two materials, a new Hf<sub>x</sub>Zr<sub>1-x</sub>Te<sub>2</sub> alloy with type-III Dirac cone emerges at x=0.2 [4] (Fig. 1d). We also provide experimental evidence that by using MBE, HfTe<sub>2</sub> [5], ZrTe<sub>2</sub> [6] and Hf<sub>0.2</sub>Zr<sub>0.8</sub>Te<sub>2</sub> [4] can be grown on InAs(111) substrates, and by using in-situ ARPES, that the Dirac point lies at -or very close to- the Fermi level (Fig. 1e). Our synchrotron ARPES results show that the Dirac cone remains unaltered as the photon energy is varied, indicating that there is no energy dispersion along the  $k_z$  axis, as expected for type-III Dirac semimetal.

We acknowledge the financial support from the European Union H2020, Contract No. 824123 -SKYTOP.

## References

- [1] G. E. Volovik and K. Zhang, J. Low Temp. Phys. 189, 276 (2017).
- [2] H. Liu et al., Phys. Rev. Lett. 120, 237403 (2018).
- [3] L. Jin et al., Phys. Rev. B 101, 045130 (2020).
- [4] S. Fragkos et al., J. Appl. Phys. 129, 075104 (2021).
- [5] S. A. Giamini et al., 2D Mater. 4, 015001 (2017).
- [6] P. Tsipas et al., ACS Nano 12, 1696 (2018).

## Figures

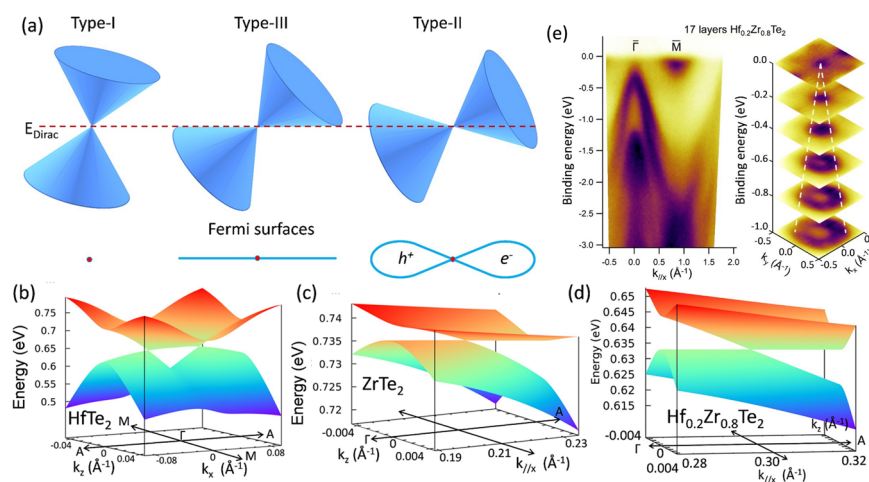


**Figure 1:** (a) Schematic illustration of the different types of DSMs. (b-d) show the energy dispersion in the  $k_z$ - $k_x$  plane near the crossings for HfTe<sub>2</sub>, ZrTe<sub>2</sub> and Hf<sub>0.2</sub>Zr<sub>0.8</sub>Te<sub>2</sub>, respectively. (e) . ARPES spectra and  $k_x$ - $k_y$  energy contour plots at different binding energies of 17 layers Hf<sub>0.2</sub>Zr<sub>0.8</sub>Te<sub>2</sub> along the  $\Gamma M$  direction of the BZ.